A&A 491, L29–L32 (2008)
DOI: 10.1051/0004-6361:200810736

Astronomy & Astrophysics

Letter to the Editor

A photometric redshift of $z = 1.8^{+0.4}_{-0.3}$ for the *AGILE* GRB 080514B⋆

A. Rossi[1], A. de Ugarte Postigo[2], P. Ferrero[1], D. A. Kann[1], S. Klose[1], S. Schulze[1], J. Greiner[3], P. Schady[4], R. Filgas[1], E. E. Gonsalves[1,5], A. Küpcü Yoldaş[3,6], T. Krühler[3,7], G. Szokoly[3,8], A. Yoldaş[3], P. M. J. Afonso[3], C. Clemens[3], J. S. Bloom[9], D. A. Perley[9], J. P. U. Fynbo[10], A. J. Castro-Tirado[11], J. Gorosabel[11], P. Kubánek[11,18], A. C. Updike[12], D. H. Hartmann[12], A. Giuliani[13], S. T. Holland[14], L. Hanlon[15], M. Bremer[16], J. French[15], G. Melady[15], and D. A. García-Hernández[17]

[1] Thüringer Landessternwarte Tautenburg, Sternwarte 5, 07778 Tautenburg, Germany
e-mail: rossi@tls-tautenburg.de
[2] European Southern Observatory, Alonso de Córdova 3107, Vitacura, Casilla 19001, Santiago 19, Chile
[3] Max-Planck-Institut für Extraterrestrische Physik, Giessenbachstrasse, 85748 Garching, Germany
[4] Mullard Space Science Laboratory, University College London, Holmbury St. Mary, Dorking, Surrey RH5 6NT, UK
[5] Darthmouth College, Hanover, NH 03755, USA
[6] European Southern Observatory, Karl-Schwarzschild-Strasse 2, 85748 Garching, Germany
[7] Universe Cluster, Technische Universität München, Boltzmannstraße 2, 85748, Garching, Germany
[8] Institute of Physics, Eötvös University, Pázmány P. s. 1/A, 1117 Budapest, Hungary
[9] Department of Astronomy, University of California, Berkeley, CA 94720-3411, USA
[10] Dark Cosmology Centre, Niels Bohr Institute, University of Copenhagen, Juliane Maries Vej 30, 2100 Copenhagen, Denmark
[11] Instituto de Astrofísica de Andalucía (IAA-CSIC), Apartado de Correos 3.004, 18080 Granada, Spain
[12] Clemson University, Department of Physics and Astronomy, Clemson, SC 29634-0978, USA
[13] INAF/IASF - Milano, via E. Bassini 15, 20133 Milano, Italy
[14] Astrophysics Science Division, Code 660.1, 8800 Greenbelt Road, Goddard Space Flight Centre, Greenbelt, MD 20771, USA
[15] School of Physics, University College Dublin, Dublin 4, Ireland
[16] Institut de Radio Astronomie Millimetrique (IRAM), 300 rue de la Piscine, 38406 Saint-Martin d'Hères, France
[17] Instituto de Astrofísica de Canarias (IAC), C/. via Láctea s/n, 38205 La Laguna (Tenerife), Spain
[18] Universidad de Valencia, Edif. Institutos de Investigación (GACE-ICMOL), Campus de Paterna, 46980 Paterna, Spain

Received 1 August 2008 / Accepted 6 October 2008

ABSTRACT

The *AGILE* gamma-ray burst GRB 080514B is the first detected to have emission above 30 MeV and an optical afterglow. However, no spectroscopic redshift for this burst is known. We report on our ground-based optical/NIR and millimeter follow-up observations of this event at several observatories, including the multi-channel imager GROND on La Silla, supplemented by *Swift* UVOT and *Swift* XRT data. The spectral energy distribution (SED) of the optical/NIR afterglow is found to decline sharply bluewards to the *UV* bands, which can be utilized in estimating the redshift. Fitting the SED from the *Swift* UVOT *uvw2* band to the *H* band, we estimate a photometric redshift of $z = 1.8^{+0.4}_{-0.3}$, which is consistent with the reported pseudo-redshift based on gamma-ray data. We find that the afterglow properties of GRB 080514B do not differ from those exhibited by the global sample of long bursts. Compared with the long burst sample, we conclude that this burst was special because of its high-energy emission properties, even though both its afterglow and host galaxy are not remarkable in any way. Obviously, high-energy emission in the gamma-ray band does not automatically correlate with the occurrence of special features in the corresponding afterglow light.

Key words. gamma rays: bursts

1. Introduction

Gamma-Ray Bursts (GRBs) are the most luminous explosions in the Universe, with the bulk of the released energy emerging in the 0.1 to 1 MeV range (e.g. Kaneko et al. 2006; Preece et al. 2000). Most bursts have not been observed at energies much above 1 MeV, where low photon counts and typically small instrumental collecting areas hamper the gathering of data. For example, the *Burst And Transient Source Experiment* (BATSE; operating from 25 keV to 2 MeV) onboard the *Compton Gamma-Ray Observatory* (CGRO) detected 2704 bursts from 1991 to 2000, while the COMPTEL telescope on CGRO, operating in the 0.8 MeV to 30 MeV range, in the same time period observed only 44 events with high significance (Hoover et al. 2005).

To our knowledge, no burst detected at energies above 30 MeV has had an observed afterglow. The discovery of GRB 080514B by the Italian *AGILE* gamma-ray satellite (Tavani et al. 2008) on May 14, 2008 at 09:55:56 UT (Rapisarda et al. 2008) was therefore of particular interest. *AGILE* carries three instruments covering the energy range from 20 keV to 50 GeV and detected GRB 080514B at energies well above 30 MeV (Giuliani et al. 2008a,b). GRB 080514B was a bright, multi-spiked event with a duration (T_{90}) of 5.6 s, which implies that it is a long burst.

The burst was also observed by *Mars Odyssey,* operating as part of the Interplanetary Network (IPN; Hurley et al. 2006),

⋆ Appendix A is only available in electronic form at http://www.aanda.org

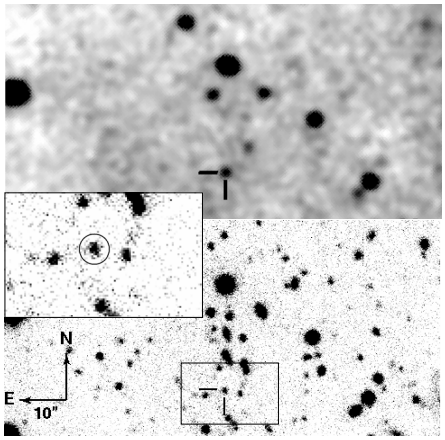

Fig. 1. *Top*: IAC80 *I*-band discovery image of the optical afterglow of GRB 080514B. The afterglow is highlighted. *Bottom*: Keck *R*-band image obtained 24 days after the trigger. The underlying host galaxy is clearly detected. The zoom inset of the Keck image shows the host galaxy.

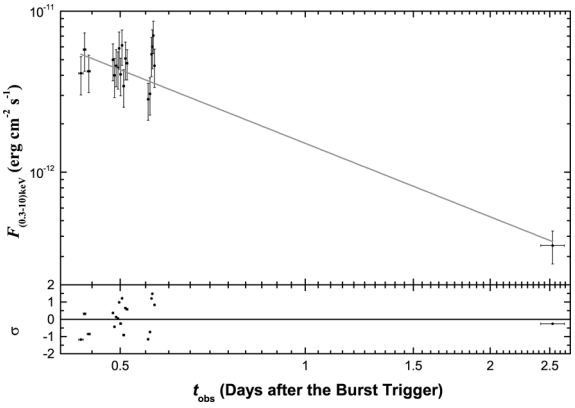

Fig. 2. The X-ray light curve of the afterglow of GRB 080514B observed by *Swift* XRT. The resulting decay index is $\alpha_X = 1.52 \pm 0.14$.

making it possible to constrain the size of the error box to about 100 arcmin^2 (Rapisarda et al. 2008). This localization led to the discovery of its X-ray afterglow by the *Swift* satellite at coordinates RA, Dec. (J2000) = $21^h31^m22\overset{s}{.}62$, $+00°42'30\overset{''}{.}3$ with an uncertainty of $1\overset{''}{.}6$ (radius, 90% confidence) at 0.43 days after the trigger (Page et al. 2008). Before the announcement of the X-ray afterglow position, however, the optical afterglow had already been discovered by our group by observing the complete IPN error box (de Ugarte Postigo et al. 2008a,b; Fig. 1). In the following we present our ground-based follow-up observations of the afterglow of GRB 080514B, supplemented by *Swift* UVOT and XRT data, starting 0.43 days after the trigger.

2. Observations and data reduction

Swift XRT data were obtained from the *Swift* data archive and the light curve from the *Swift* light curve repository (Evans et al. 2007). To reduce the data, the software package `HeaSoft` 6.4 was used[1] with the calibration file version `v011`. Data analysis was performed following the procedures described in Nousek et al. (2006). Spectral analysis was completed with the software package `Xspec v12`, using the elemental abundance templates of the Galactic interstellar medium given by Wilms et al. (2000).

Swift UVOT observed the field in the broad-band *v*, *b*, *u*, *uvw*1, *uvm*2, and *uvw*2 lenticular filters (Holland 2008; for the filter definitions, see Poole et al. 2008). A second set of observations were obtained in the *white* band about 2.5 days after the trigger. Photometry of these data was performed using the standard *Swift* software tool *uvotmaghist* (version 1.0) and following the procedures described in Poole et al. (2008).

Ground-based follow-up observations were performed by our group using the 16″ Watcher telescope in South Africa, the IAC80 telescope at Observatorio del Teide, the MPG/ESO 2.2 m telescope equipped with GROND (Greiner et al. 2007, 2008), the Nordic Optical Telescope, the Kitt Peak 4 m telescope, the Gemini North 8 m and the Keck 10 m telescope. The data were analyzed using standard PSF photometry, and only in analyzing the host galaxy was aperture photometry applied (Table A.1).

Our data set was completed by an observation at 86 GHz with the Plateau de Bure interferometer (Guilloteau et al. 1992) using the 5-antenna compact D configuration, performed 3.92 days after the burst. We detected no source at the afterglow position to within a 3-sigma detection limit of 0.57 mJy.

[1] `http://heasarc.gsfc.nasa.gov/docs/software/lheasoft`

3. Results

Since GRB 080514B is the first burst to have both detected high energy emission and a known afterglow, we are particularly interested in two points: (a) do the afterglow properties separate this burst from the long burst sample? (b) what is its photometric redshift? While the former question is related to whether burst properties correlate with afterglow features, the latter is critical in quantifying the energetics of the burst.

3.1. The afterglow

X-ray data: because *Swift* did not begin observations until 0.43 days after the SuperAGILE/IPN detection, the quality of both the spectrum and the light curve of the X-ray afterglow suffer from a low count rate and data gaps due to *Swift*'s orbit. Fitting the afterglow X-ray spectrum of the first observing block (0.43–0.54 days; total exposure time 5916 s) with an absorbed power-law, results in a spectral slope (writing the flux density as $F_\nu(t) \propto t^{-\alpha}\nu^{-\beta}$) of $\beta_X = 1.01^{+0.28}_{-0.25}$ and an effective hydrogen column density of $N_H = 1.4^{+0.9}_{-0.8} \times 10^{21}$ cm^{-2} (χ^2/d.o.f. = 7.97/9; 1σ uncertainties), in agreement with results reported by Page et al. (2008; Fig. A.2). No constraints on a possible spectral evolution could be set. The derived hydrogen column density is higher than the Galactic value of $N_H = 0.375 \times 10^{21}$ cm^{-2} based on radio observations (Kalberla et al. 2005). This implies that additional absorption by gas occurs inside the GRB host galaxy. We note, however, that the error bars are large.

The canonical X-ray afterglow light curve derived by Nousek et al. (2006) shows a transition from a plateau to a normal decay phase between about 0.1 and 1 days post-burst and a jet break thereafter. Unfortunately, for GRB 080514B at early times (0.43 to 0.54 days) the X-ray light curve exhibits substantial scatter, as has also been the case for other X-ray afterglows (cf. O'Brien et al. 2006). This, and the lack of data thereafter, makes it impossible to decide whether there was a plateau phase at early times (0.43 to 0.54 days), a flare, or a break in the decay between 0.54 and 2.5 days. Assuming a simple power-law decay, the light curve is well described by a temporal decay index of $\alpha_X = 1.52 \pm 0.14$ (χ^2/d.o.f. = 17.68/18). A smoothly broken power-law is statistically unlikely (Fig. 2). The spectral fit was then used to derive an energy conversion factor of 6.1×10^{-11} erg cm^{-2} counts^{-1}.

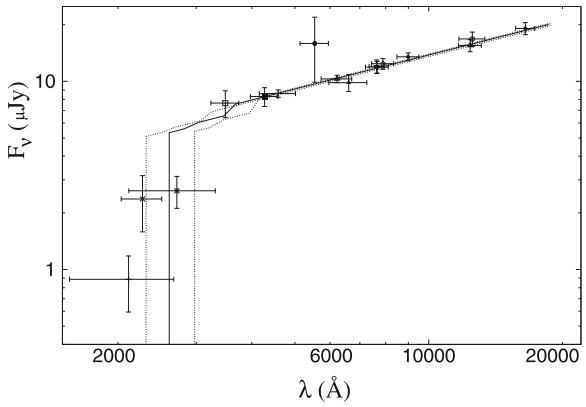

Fig. 3. The SED of the afterglow at 1 day after the burst fitted using the *HyperZ* tool (solid line; the dotted lines show the 1σ uncertainties). *From left to right*: UVOT *uvw*2, *uvm*2, *uvw*1, *u* and *b*, GROND g', UVOT *v*, GROND r', R_C, GROND i', Gemini i', I_C, GROND z', GROND *J*, NEWFIRM *J* (see Table A.1) and GROND *H*. The widths of the bands correspond to their approximation by a Gaussian filter (see Bolzonella et al. 2000). The UVOT *v* band is affected by a short exposure time, the low sensitivity of the detector at longer wavelengths and high background.

Optical data: afterglow coordinates were derived from the GROND first epoch stacked r'-band image, which has an astrometric precision of about 0.″2, corresponding to the rms accuracy of the USNO-B1 catalogue (Monet et al. 2003). The coordinates of the optical afterglow are RA, Dec. (J2000) = $21^{\rm h}31^{\rm m}22\overset{\rm s}{.}69$, $+00°42'28\overset{''}{.}6$ (Galactic coordinates l, b = $54\overset{\circ}{.}57$, $-34\overset{\circ}{.}49$). Magnitudes were corrected for extinction according to the interstellar extinction curve provided by Cardelli et al. (1989) and by assuming both a colour excess $E(B-V) = 0.06$ (Schlegel et al. 1998) and $R_V = 3.1$.

While the optical afterglow is detected in a broad range of filters, from the *Swift* UVOT *uvw*2 band to the *H* band (160–1700 nm), the data set is sparse with some scatter (Fig. A.1). To determine the slope of the light-curve decay as well as the spectral energy distribution (SED) of the afterglow, we simultaneously fit all 14 photometric bands exhibiting detections with a single power-law (excluding the UVOT *white* filter measurement) and an added host component for those bands in which the late flattening indicates that the afterglow has become fainter than the host. From this fit (χ^2/d.o.f. = 1.51/25), we find a decay slope $\alpha_{\rm opt} = 1.67 \pm 0.07$. Unfortunately, this value alone is insufficient to decide whether this is a pre-break or a post-break decay. Light curves with such a (steep) pre-jet break decay slope or with such a (flat) post-jet break decay slope have both been observed (for compilations of optical afterglow data see, e.g. Zeh et al. 2006; Kann et al. 2008). We therefore find no evidence for a jet break.

3.2. SED and photometric redshift

The simultaneous fitting procedure described in Sect. 3.1 yields magnitudes normalized to one day after the GRB for each band, which define the SED of the afterglow. We find no evidence for chromatic evolution but caution again that the data are sparse and is often of low signal-to-noise ratio. The SED is described well by a simple power-law with spectral slope $\beta_{\rm opt} = 0.64 \pm 0.03$ (χ^2/d.o.f. = 8.58/10) from the *H* band to the *U* band (Fig. 3). We do not find evidence for dust in the host galaxy, which would create spectral curvature. On the other hand, the three UVOT UV filters show a much steeper slope, which we attribute to intergalactic Lyman dropout.

Table 1. Predicted temporal slopes α for various afterglow scenarios based on the measured spectral slopes $\beta_{\rm opt} = 0.64 \pm 0.03$ (Sect. 3.2) and $\beta_{\rm X} = 1.01^{+0.28}_{-0.25}$ (Sect. 3.1). These values have to be compared with the measured $\alpha_{\rm opt} = 1.67 \pm 0.07$ and $\alpha_{\rm X} = 1.52 \pm 0.14$. Assuming a jet, for $t < t_{\rm break}$ the isotropic model holds, whereas for $t > t_{\rm break}$ the jet model applies (e.g. Zhang & Mészáros 2004). The σ-level represents the difference between the predicted and the observed temporal slope, normalized to the square root of the sum of their quadratic errors. The favoured model is highlighted.

Afterglow model	Optical		X-ray	
	$\alpha_{\rm opt}$	σ-level	$\alpha_{\rm X}$	σ-level
Iso				
ISM, wind, $\nu_{\rm c} < \nu$	0.46 ± 0.05	−14.54	$1.02^{+0.42}_{-0.38}$	−1.14
ISM, $\nu < \nu_{\rm c}$	0.96 ± 0.05	−8.53	$1.52^{+0.42}_{-0.38}$	−0.01
wind, $\nu < \nu_{\rm c}$	1.46 ± 0.05	−2.52	$2.02^{+0.42}_{-0.38}$	1.24
Jet				
ISM, wind, $\nu_{\rm c} < \nu$	1.28 ± 0.06	−4.23	$2.02^{+0.56}_{-0.50}$	0.96
ISM, wind, $\nu < \nu_{\rm c}$	2.28 ± 0.06	6.62	$3.02^{+0.56}_{-0.50}$	2.89

Using *HyperZ* (Bolzonella et al. 2000) and assuming $A_{\rm V}^{\rm host} = 0$, the best fit solution provides a photometric redshift of $z = 1.8^{+0.4}_{-0.3}$ (1σ uncertainties, see Avni 1976), in agreement with the constraint of $z < 2.3$ based on Gemini-North observations (Perley et al. 2008) and the pseudo-redshift of $z = 1.76 \pm 0.30$ based on the burst spectrum (Pelangeon & Atteia 2008). On the other hand, it is intermediate between the two redshift estimations presented by Gendre et al. (2008). Exclusion of the *uvw*2 filter from the fit did not alter the obtained photometric redshift. The doubling of the assumed Galactic reddening to $E(B-V) = 0.12$ also did not change the deduced photometric redshift significantly, although in this case the shape of the SED clearly indicated that we had overcorrected for extinction.

Using the derived redshift $z = 1.8$ and the prompt emission properties as measured by *Konus-Wind* (Golenetskii et al. 2008), we find a bolometric isotropic energy release of $E_{\rm iso} = (2.63^{+0.22}_{-0.23}) \times 10^{53}$ erg and a peak luminosity of $L_{\rm iso} = (4.73 \pm 0.99) \times 10^{53}$ erg s^{-1}, which are high but not exceptional values. The host-frame peak energy of $E_{\rm peak} = 627^{+64}_{-62}$ keV is unremarkable. Therefore, it is possible that the *AGILE* detection at high energies is of such high significance because of the high luminosity of this event.

Fixing $z = 1.8$, we refit the SED (now excluding the *UVOTUV* filters) with dust models for the Milky Way, Large and Small Magellanic Clouds (for the procedure, see Kann et al. 2006). In all cases, adding A_V as an additional parameter does not improve the fits significantly, and the derived extinction is also zero within errors in all three cases (at 3σ confidence, $A_V \leq 0.06$ for MW, ≤0.17 for LMC, and ≤0.14 for SMC dust). No evidence for a 2175 Å feature (which would lie close to the R_C and r' bands) is apparent, and no discrimination is possible between dust models. The assumption of zero extinction is consistent with several studies (Starling et al. 2007; Schady et al. 2007) on the dust-to-gas ratios in GRB host galaxies.

By fixing the Galactic hydrogen column density to the value given by Kalberla et al. (2005), and setting $z = 1.8$, we infer that $N_{\rm H}^{\rm host} = 8.7^{+9.0}_{-7.3} \times 10^{21}$ cm^{-2} and obtain an unabsorbed spectral index of $\beta_{\rm X} = 0.94^{+0.24}_{-0.21}$ (χ^2/d.o.f. = 8.12/9). While the deduced $N^{\rm host}$ allows potentially for a substantial host extinction, we note that within the large 1σ errors this result is not in conflict with the non-detection of host extinction in the optical bands. The

measured spectral slope is consistent with the mean value found for *Swift* X-ray afterglows (O'Brien et al. 2006). Using the derived spectral slope and redshift, the absolute magnitude of the afterglow is $M_B = -22.17 \pm 0.2$ and $M_B = -20.17 \pm 0.5$, at one and four days after the GRB, respectively (for the method see Kann et al. 2006, 2008; no extinction is assumed). These are typical values for a GRB afterglow, i.e. GRB 080514B is neither exceptionally bright or faint.

As mentioned in Sect. 3.1, based on the light curve alone we cannot decide whether the data belong to the pre-jet break phase or to the post-jet break phase. Using the α–β relations (Zhang & Mészáros 2004), the optical/NIR data at 1 day are consistent with a wind model with the cooling frequency bluewards of the optical/NIR bands and a light curve in the pre-break regime (Table 1 and Fig. A.3). The much larger error bars in the X-ray data are less of a constraint here. Unfortunately, the non-detection of the afterglow at 86 GHz does not help to constrain the shape of the SED.

3.3. The host galaxy

A galaxy underlying the position of the optical transient is detected in all GROND optical bands at 8.9 days as well as in the deep Keck g and R-band images obtained 24.13 days post-burst. Using the stacked GROND $g'r'i'z'$ images, its coordinates are RA, Dec. (J2000) = $21^{\rm h}31^{\rm m}22\overset{\rm s}{.}68$, $+00°42'28\overset{''}{.}8$, which is offset by $0\overset{''}{.}3 \pm 0\overset{''}{.}2$ from the position of the optical afterglow. Assuming a cosmological model with $H_0 = 71\ {\rm km\,s^{-1}\ Mpc^{-1}}, \Omega_M = 0.27, \Omega_\Lambda = 0.73$ (Spergel et al. 2003), for $z = 1.8$ the offset of the optical transient from the centre of this galaxy is 2.6 ± 1.7 kpc.

By assuming a power-law spectrum for the putative host galaxy of the form $F_\nu \propto \nu^{-\beta_{\rm gal}}$, its absolute R-band magnitude is $M_R = m_R - \mu - k$, where $\mu = 45.70$ mag is the distance modulus and k is the cosmological k-correction, $k = -2.5(1 - \beta_{\rm gal}) \log(1 + z)$. For $\beta_{\rm gal} = 0.45$, as it follows from the third epoch GROND $g'r'i'z'$ data, this galaxy has $M_R = -20.9$, which is about 0.5 mag more luminous than the characteristic magnitude of the Schechter r-band luminosity function of galaxies in the Las Campanas redshift survey (Lin et al. 1996). Its R-band magnitude agrees well with the distribution of long-burst host magnitudes for this redshift (Guziy et al. 2005; Savaglio et al. 2008).

4. Summary and conclusions

To our knowledge, GRB 080514B is the first burst detected above 30 MeV for which an afterglow has been found in the X-ray band and in the optical/NIR bands. Based on the presented follow-up observing campaign, we have found that: (1) the X-ray/optical/NIR light curve after 0.4 days is well described by a single power-law with no sign of a jet break; (2) the SED of the afterglow indicates strong Lyman blanketing at short wavelengths, implying a photometric redshift of $z = 1.8^{+0.4}_{-0.3}$. This is the first redshift determination for a GRB with prompt emission detected at energies of above 30 MeV. We have found no evidence for extinction by dust in the GRB host galaxy; (3) by comparing the observed light curve decay with the SED, we infer a model scenario in which the afterglow blast wave propagated into a wind medium; (4) the intrinsic properties of the optical afterglow are typical of long-duration GRBs; (5) the putative host galaxy has $R_{\rm c} = 24.2 \pm 0.3$ and an absolute R-band magnitude of $M_R = -20.9 \pm 0.3$. The optical transient was offset from the centre of its host by 2.6 ± 1.7 kpc.

According to our data set, we conclude that the afterglow and the host properties correlate well with the corresponding properties of long burst events. The only property that is remarkable about this burst is its detection above 30 MeV. In principle, our data are consistent with a scenario in which the physical processes that create a GRB are independent of those that generate the afterglow light (e.g. Zhang & Mészáros 2004). While we must await further events and the acquisition of far higher quality data sets before being able to deduce reliable conclusions, it is clear that the diversity observed in the high-energy properties of the bursts reveals more unanswered questions about the nature of afterglows.

Acknowledgements. We thank the referee for a very careful reading of the manuscript and a rapid reply. A.R., P.F. and S.K. acknowledge support by DFG Kl 766/11-3, A. D. U. P. by an ESO fellowship, D. A. K., S. S., and R. F. by the Thüringer Landessternwarte, T. K. by the DFG cluster of excellence "Origin and Structure of the Universe", J. P. U. F. by the DNRF, J. Gorosabel by the programmes ESP2005-07714-C03-03 and AYA2007-63677, and L. H. by SFI. We thank D. Malesani for a careful reading of the manuscript, P. E. Nissen and W. J. Schuster for performing the NOT observations as well as A. Pimienta, E. Curras and C. Pereira for performing the IAC80 observations. This work made use of data supplied by the UK Swift Science Data Centre at the University of Leicester.

References

Avni, Y. 1976, ApJ, 210, 642
Bolzonella, M., Miralles, J.-M., & Pelló, R. 2000, A&A, 363, 476
Cardelli, J. A., Clayton, G. C., & Mathis, J. S. 1989, ApJ, 345, 245
Evans, P. A., Beardmore, A. P., Page, K. L., et al. 2007, A&A, 469, 379
de Ugarte Postigo, A., Castro-Tirado, A., Gorosabel, J., et al. 2008a, GCN, 7719
de Ugarte Postigo, A., Castro-Tirado, A., & Gorosabel, J., et al. 2008b, GCN, 7720
Gendre, A., Galli, A., & Boër, M. 2008, GCN, 7730
Giuliani, A., Fornari, F., Mereghetti, S., et al. 2008a, GCN, 7716
Giuliani, A., Mereghetti, S., Fornari, F., et al. 2008b, A&A, 491, L25
Golenetskii, S., Aptekar, R., & Mazets, E. 2008, GCN, 7751
Greiner, J., Bornemann, W., Clemens, C., et al. 2007, The Messenger, 130, 12
Greiner, J., Bornemann, W., Clemens, C., et al. 2008, PASP, 120, 405
Guilloteau, S., Delannoy, J., Downes, D., et al. 1992, A&A, 262, 624
Guziy, S., Gorosabel, J., Castro-Tirado, A. J., et al. 2005, A&A 441, 975
Holland, S. T. 2008, GCN, 7759
Hoover, A. S., Kippen, R. M., & McConnell, M. L. 2005, N. Cim. 28 C, 4, 825
Hurley, K., Mitrofanov, I., Kozyrev, A., et al. 2006, ApJS, 164, 124
Kalberla, P. M. W., Burton, W. B., Hartmann, D., et al. 2005, A&A, 440, 775
Kaneko, Y., Preece, R. D., Briggs, M. S., et al. 2006, ApJS, 166, 298
Kann, D. A., Klose, S., Zeh, A., et al. 2006, ApJ, 641, 993
Kann, D. A., Klose, S., Zhang, B., et al. 2008, ApJ, submitted [arXiv:0712:2186]
Lin, H., Kirshner, R. P., Shectman, S. A., et al. 1996, ApJ, 464, 60
Malesani, D., Nissen, P. E., Schuster, W., J., et al. 2008, GCN, 7734
Monet, D. G., Levine, S. E., Canzian, B., et al. 2003, AJ, 125, 984
Nousek, J. A., Kouveliotou, C., Grupe, D., et al. 2006, ApJ, 642, 389
O'Brien, P. T., Willingale, R., Osborne, J., et al. 2006, ApJ, 647, 1213
Page, K. L., Beardmore, A. P., Mereghetti, S., et al. 2008, GCN, 7723
Pélangeon, A., & Atteia, J.-L. 2008, GCN, 7760
Perley, D. A., Bloom, J. S., Chen, H.-W., et al. 2008, GCN, 7874
Poole, T. S., Breeveld, A. A., Page, M. J., et al. 2008, MNRAS, 383, 627
Preece, R. D., Briggs, M. S., Mallozzi, R. S., et al. 2000, ApJS, 126, 19
Rapisarda, M., Costa, E., Del Monte, E., et al. 2008, GCN, 7715
Rossi, A., Küpcü Yoldaş, A., Greiner, J., et al. 2008a, GCN, 7722
Rossi, A., Küpcü Yoldaş, A., Greiner, J., et al. 2008b, GCN, 7724
Schlegel, D., Finkbeiner, D. P., & Davis, M. 1998, ApJ, 500, 525
Savaglio, S., Glazebrook, K., Le Borgne, D. 2008 [arXiv:0803.2718v1]
Schady, P., Mason, K. O., Page, M. J., et al. 2007, MNRAS, 377, 273
Spergel, D. N., Verde, L., Peiris, H. V., et al. 2003, ApJS, 148, 175
Starling, R. L. C., Wijers, R. A. M. J., Wiersema, K., et al. 2007, ApJ, 661, 787
Tavani, M., Barbiellini, G., Argan, A., et al. 2008 [arXiv:0807.4254]
Updike, A. C., Bryngelson, G., & Hartmann, D. H. 2008a, GCN, 7725
Updike, A. C., Bryngelson, G., & Hartmann, D. H. 2008b, GCN, 7745
Wilms, J., Allen, A., & McCray, R. 2000, ApJ, 542, 914
Zeh, A., Klose, S., & Kann, D. A. 2006, ApJ, 637, 889
Zhang, B., & Mészáros, P. 2004, Int. J. Mod. Phys. A, 19, 2385

Appendix A: Observational data and the SED of the afterglow

Table A.1. Log of observations.

Time (days)	Filter	Instr./Telesc.	Exposure (s)	Magnitudes
0.430	*uvw1*	UVOT	284	20.45 ± 0.40
0.432	*u*	UVOT	142	19.75 ± 0.30
0.434	*b*	UVOT	142	21.00 ± 0.63
0.438	*uvw2*	UVOT	568	21.47 ± 0.56
0.443	*v*	UVOT	142	>20.9
0.446	*uvm2*	UVOT	413	>22.0
0.488	*uvw1*	UVOT	419	20.17 ± 0.27
0.492	*u*	UVOT	209	19.91 ± 0.27
0.494	*b*	UVOT	209	20.40 ± 0.31
0.501	*uvw2*	UVOT	838	21.78 ± 0.57
0.507	*v*	UVOT	209	19.74 ± 0.42
0.512	*uvm2*	UVOT	616	20.63 ± 0.37
0.555	*uvw1*	UVOT	415	20.88 ± 0.46
0.559	*u*	UVOT	207	20.09 ± 0.32
0.561	*b*	UVOT	207	21.62 ± 0.91
0.567	*uvw2*	UVOT	791	22.09 ± 0.76
0.640	R_C	Watcher	120 × 14	19.23 ± 0.47
0.660	R_C	Watcher	120 × 15	19.89 ± 0.56
0.727	I_C	IAC 80	3 × 300	20.26 ± 0.21
0.743	I_C	IAC 80	3 × 300	20.59 ± 0.20
0.761	I_C	IAC 80	3 × 300	20.16 ± 0.16
0.774	I_C	IAC 80	3 × 300	20.03 ± 0.14
0.907	g'	GROND/2.2 m	3 × 1501	21.53 ± 0.04
0.907	r'	GROND/2.2 m	3 × 1501	21.16 ± 0.03
0.907	i'	GROND/2.2 m	3 × 1501	20.77 ± 0.08
0.907	z'	GROND/2.2 m	3 × 1501	20.43 ± 0.05
0.907	*J*	GROND/2.2 m	3 × 1200	19.82 ± 0.03
0.907	*H*	GROND/2.2 m	3 × 1200	19.10 ± 0.04
0.907	*K*	GROND/2.2 m	2 × 1200	>17.5
1.021	*J*	NEWFIRM/KPNO	23 × 30 × 2	19.84 ± 0.14
1.038	*J*	NEWFIRM/KPNO	15 × 30 × 2	20.06 ± 0.07
1.763	R_C	NOT	1 × 300	22.31 ± 0.08
1.782	*B*	NOT	1 × 300	23.03 ± 0.13
1.798	I_C	NOT	1 × 300	22.00 ± 0.10
1.899	i'	GMOS/Gemini	1 × 200	21.83 ± 0.06
1.993	g'	GROND/2.2 m	1 × 1501	22.74 ±0.08
1.993	r'	GROND/2.2 m	1 × 1501	22.38 ± 0.10
1.993	i'	GROND/2.2 m	1 × 1501	21.78 ± 0.13
1.993	z'	GROND/2.2 m	1 × 1501	>21.6
1.993	*J*	GROND/2.2 m	1 × 1200	>20.3
1.993	*H*	GROND/2.2 m	1 × 1200	>19.1
1.993	*K*	GROND/2.2 m	1 × 1200	>17.7
2.023	*J*	NEWFIRM/KPNO	15 × 30 × 2	20.95 ± 0.30
2.039	*H*	NEWFIRM/KPNO	15 × 15 × 4	>20.3
2.536	*white*	UVOT	5361	22.19 ± 0.17
8.965	g'	GROND/2.2 m	4 × 1501	24.05 ± 0.17
8.965	r'	GROND/2.2 m	4 × 1501	24.40 ± 0.25
8.965	i'	GROND/2.2 m	4 × 1501	23.35 ± 0.26
8.965	z'	GROND/2.2 m	4 × 1501	23.28 ± 0.24
8.965	*J*	GROND/2.2 m	4 × 1200	>21.9
8.965	*H*	GROND/2.2 m	4 × 1200	>20.5
8.965	*K*	GROND/2.2 m	3 × 1200	>18.4
24.13	R_C	Keck	960	24.17 ± 0.33
24.13	g'	Keck	1080	24.73 ± 0.34

The first column provides the mid-time in days after the GRB. Vega magnitudes are not corrected for Galactic extinction. The upper limits are 3σ above the background. The data given in the table supersede the corresponding magnitudes reported in de Ugarte Postigo et al. (2008a,b), Rossi et al. (2008a,b), Updike et al. (2008a,b), Malesani et al. (2008), and Perley et al. (2008).

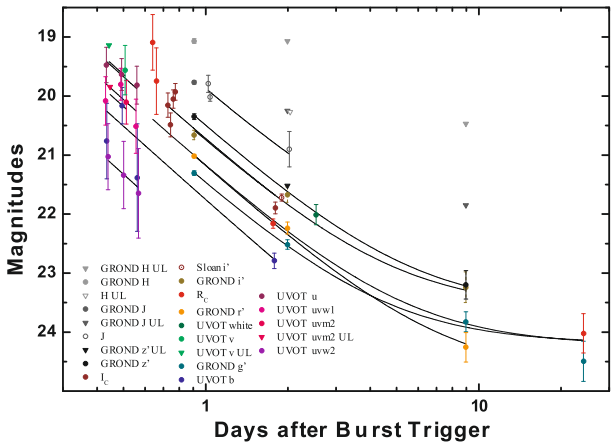

Fig. A.1. The light curve of the optical/NIR afterglow of GRB 080514B. The afterglow is detected in all bands (*uvw2* to *H*) except *K*. Upper limits are given as downward pointing triangles. The lines show the simultaneous fit with a single power-law plus host galaxy component. The decay slope is $\alpha_{\rm opt} = 1.67 \pm 0.07$. UL stands for upper limit.

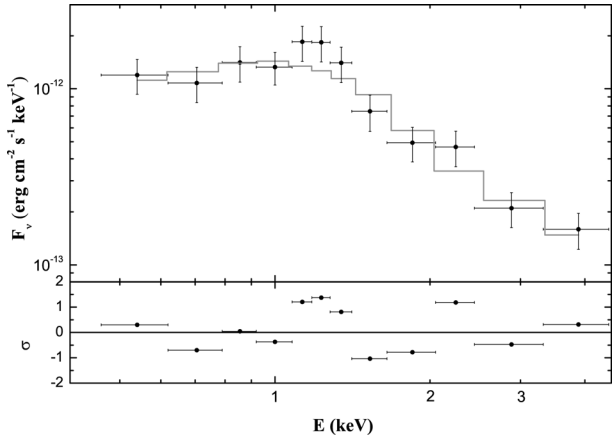

Fig. A.2. The observed X-ray spectrum of the afterglow of GRB 080514B obtained in photon counting mode at 0.5 days. The spectrum was fitted with an absorbed power-law and a gas column density of 1.4×10^{21} cm^{-2} (Sect. 3.1). The *lower panel* shows the residuals of the fit computed to be the difference between the observed data and the best-fit model, normalized to the error in the observed data.

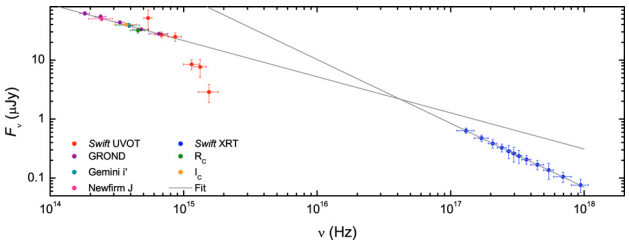

Fig. A.3. The broad-band SED of the afterglow of GRB 080514B at 0.5 days after the burst in the observer frame after correction for extinction by dust (optical data; Sect. 3.2) and for absorption by a gas column density of 1.4×10^{21} cm^{-2} (X-ray data; Sect. 3.1), assuming no additional contribution from the ISM in the GRB host galaxy. The straight lines show the spectral slopes $\beta_{\rm opt}$ from the *H* band to the *U* band (Sect. 3.2) at 1 day and $\beta_{\rm X}$ at 0.5 days (Sect. 3.1), and thereby we assumed that $\beta_{\rm opt}$ did not change between 0.5 days and 1 day after the burst. The bandwidths of the optical/NIR data shown here correspond to their true transmission curves, in contrast to the Gaussian approximation we have shown in Fig. 3. We note in particular that the large 1σ uncertanties of the spectral slope in the X-ray band (Sect. 3.1) are not shown here. The position of the cooling frequency is therefore far less tightly constrained than implied by this plot.